

Beyond the Boltzmann equation for weakly coupled quantum fields

Xu-Yao Hu¹ and Vladimir Rosenhaus²

¹ *Institute for Advanced Study, Tsinghua University,
Beijing, China*

² *Initiative for the Theoretical Sciences
The Graduate Center, CUNY
365 Fifth Ave, New York, NY*

We study the kinetic theory of a weakly interacting quantum field. Assuming a state that is close to homogeneous and stationary, we derive a closed kinetic equation for the rate of change of the occupation numbers, perturbatively in the coupling. For a dilute gas, this reproduces the quantum Boltzmann equation, which only accounts for two-to-two scattering processes. Our expression goes beyond this, with terms accounting for multi-particle scattering processes, which are higher order in the density.

September 3, 2025

Contents

1. Introduction	1
2. Keldysh contour propagators	4
3. Correlation functions and the kinetic equation	9
3.1. Tree-level kinetic equation	10
3.2. One-loop-level kinetic equation	11
3.3. Higher loop diagrams	14
4. Discussion	19
A. Contour-ordered propagators	20
B. Perturbative computation of equal-time correlation functions	22
C. Particle number non-conserving interactions	24
C.1. Next-to-leading order kinetic equation for $\lambda\phi^4$ theory	26

1. Introduction

The Boltzmann equation is the backbone of kinetic theory, compactly describing the rate of change of the density $n(x, \vec{k}_1, t)$ of particles with momentum \vec{k}_1 at position x [1, 2],

$$\left(\frac{\partial}{\partial t} + \frac{\vec{k}_1}{m} \cdot \nabla \right) n_1 = - \int d^d k_2 d^d k_3 d^d k_4 |\mathcal{A}|^2 (n_1 n_2 - n_3 n_4) \delta^{d+1}(k_{12;34}), \quad (1.1)$$

where $n_i \equiv n(x, \vec{k}_i, t)$, d is the spatial dimension, the delta function enforces both momentum and energy conservation, with $k_{12;34} \equiv k_1 + k_2 - k_3 - k_4$, and \mathcal{A} is the scattering amplitude. The equation is conceptually transparent: the density of particles with momentum k_1 decreases when a particle with momentum k_1 collides with another of momentum k_2 , producing outgoing particles with momenta k_3, k_4 . The probability of this process is proportional to the square of the scattering amplitude multiplied by the number of incoming particles at position x , and the process is summed over possible momenta of the ingoing and outgoing particles. The time-reverse process increases $n(x, \vec{k}_1, t)$.

The validity of the Boltzmann equation hinges on the assumption that the dominant interactions involve two-to-two scattering events with minimal overlap. Higher-order corrections, which scale with higher powers of the density, become particularly significant in low dimensional systems due to memory effects arising from multiple correlated collisions [3–7]. Higher order terms will

involve multi-particle scattering amplitudes [8–14], and it is challenging to write a systematic, simple, and useful higher order equation.

At first pass, the quantum Boltzmann equation is a simple modification of its classical counterpart. It accounts for the quantum attraction/repulsion of bosons/fermions, respectively, by adding a factor of $1 \pm n_i$ for the outgoing particles,

$$\left(\frac{\partial}{\partial t} + \frac{\vec{k}_1}{m} \cdot \nabla\right) n_1 = - \int d^d k_2 d^d k_3 d^d k_4 |\mathcal{A}|^2 \left(n_1 n_2 (1 \pm n_3) (1 \pm n_4) - (1 \pm n_1) (1 \pm n_2) n_3 n_4 \right) \delta^{d+1}(k_{12;34}) \quad (1.2)$$

Of course, this equation assumes a quasi-classical limit; quantum particles do not have a well-defined position and momentum. Concretely, it assumes that the state is close to homogenous in both space and time (close to stationary), in order to minimize the impact of the uncertainty relation.

More formally, a standard derivation of the quantum kinetic equation begins with the Schwinger-Dyson equations for the Green's function and self-energy on a Keldysh contour. These equations are inherently bilocal in space and time. To transform them into a closed equation for the Green's function $G(x_1, x_2)$, one typically works in the weak-coupling regime. Achieving a local form like (1.2) requires a quasi-classical approximation, which formally involves a gradient expansion in terms of $x_1 + x_2$ and the momentum, defined as the Fourier transform of $x_1 - x_2$.

In this paper we assume, at the outset, a Hamiltonian with weakly coupled interactions and a state that is spatially homogenous, nearly stationary, and close to Gaussian. The latter assumption (on the state) allows for a quantum kinetic equation that is manifestly local in time. The former assumption (on the coupling) allows for a straightforward and systematic derivation of the higher order terms (in the coupling) in the quantum kinetic equation. The derivation will be no harder (and the result more conceptually transparent) than the derivation of the classical wave kinetic equation, found perturbatively in the nonlinearity for weakly interacting waves in Ref. [15–17], which served as motivation for this work. We will give simple rules for writing down contributions to the kinetic equation at any order in the coupling, and each term will have as intuitive an interpretation as the tree-level quantum Boltzmann equation (1.2), but will now involve multiple scatterings.

One way to derive the classical wave kinetic equation is by utilizing the equations of motion to relate the occupation number, $n_k = \langle a_k^\dagger a_k \rangle$ to the equal-time four-point correlation function [18]:

$$\frac{\partial n_1}{\partial t} = 4 \text{Im} \int d^d k_2 d^d k_3 d^d k_4 \delta(\vec{k}_{12;34}) \lambda_{1234} \langle a_1^\dagger a_2^\dagger a_3 a_4 \rangle, \quad (1.3)$$

where λ_{1234} is a general, and potentially momentum-dependent, quartic interaction. The correlation function on the right-hand side is computed self-consistently in a state that is close to Gaussian, having occupation numbers n_k , and close to stationary.

There are multiple choices for what is being averaged over in the classical correlation function

on the right-hand side of (1.3). The first is over the phases of the a_k for the modes not entering the correlator [15, 19], analogous to the phase-space averaging common in deriving the Boltzmann equation. The second, which is the simplest at the technical level, is to modify the equations of motion by adding a Gaussian-random forcing and dissipation for each mode, whose magnitudes are then taken to zero while maintaining a ratio set by the desired n_k [20, 16]. Physically, this artificially mimics the coupling that a mode has to the many other modes which act as a bath. A third averaging is to take the initial state of the field a_k to be Gaussian, with variance n_k [21, 22]. All three of these averaging procedures give the same results for the (late-time) kinetic equation.

Our derivation of the quantum kinetic equation will start by reinterpreting (1.3) as a quantum equation. The correlation function on the right-hand side will be computed perturbatively in the coupling using a path integral approach. Since it is an expectation value (also known as an in-in correlator), the time in the path integral will run over a Keldysh contour. Averaging over Gaussian initial conditions will correspond to imposing boundary conditions on the Green's function. Alternatively, we can instead average over infinitesimal random forcing combined with dissipation, which is accounted for by coupling the fields on the two branches of the Keldysh contour. To give a flavor of the higher-order terms: accounting for one-loop diagrams gives,

$$\frac{\partial n_1}{\partial t} = 16\pi \int d^d k_2 d^d k_3 d^d k_4 \lambda_{1234}^2 \left((n_1+1)(n_2+1)n_3n_4 - (n_3+1)(n_4+1)n_1n_2 \right) (1 + 2\mathcal{L}_+ + 8\mathcal{L}_-) \delta(\omega_{k_1 k_2; k_3 k_4}) \delta(\vec{k}_{12;34}), \quad (1.4)$$

where ω_k is the frequency and \mathcal{L}_\pm are principal value integrals,

$$\mathcal{L}_+ = 2 \int d^d k_5 d^d k_6 \frac{\lambda_{5612} \lambda_{3456}}{\lambda_{1234}} \frac{n_5 + n_6 + 1}{\omega_{k_1 k_2; k_5 k_6}} \delta(\vec{k}_{12;56}), \quad \mathcal{L}_- = 2 \int d^d k_5 d^d k_6 \frac{\lambda_{3516} \lambda_{4625}}{\lambda_{1234}} \frac{n_6 - n_5}{\omega_{k_1 k_6; k_3 k_5}} \delta(\vec{k}_{16;35}). \quad (1.5)$$

Throughout the paper we will assume the state is homogenous — if one wishes to generalize, the left-hand side can be replaced with $\partial_t \rightarrow \partial_t + \vec{v} \cdot \vec{\nabla}$, as is standard in the Boltzmann equation.

At weak coupling, the \mathcal{L}_\pm terms may be neglected, as they are of order λ , and the scattering amplitude at leading order is λ_{1234} , so this reduces to the standard quantum Boltzmann equation (1.2), where the spatial derivatives on the left-hand side are absent due to the assumption of homogeneity. If one interprets (1.4) as a quantum Boltzmann equation computed to higher order in the density, then the terms in \mathcal{L}_\pm involving n_i represent such higher order terms, whereas the 1 in \mathcal{L}_+ contributes to a higher order in coupling correction to the scattering amplitude. Taking the large $n_i \gg 1$ limit, this equation reduces to the next-to-leading order classical wave kinetic equation [15, 16].

The paper is organized as follows: In Sec. 2 we set up the Keldysh contour for computing correlation functions and derive the propagators. In Sec. 3 we compute equal-time correlation functions perturbatively in the coupling, which via the quantum version of (1.3), gives the kinetic

equation. This is done at tree level in Sec. 3.1 and at one loop in Sec. 3.2. In Sec. 3.3 we give rules for writing the answer to arbitrary order. We conclude in Sec. 4. Appendix A reviews properties of propagators on the Keldysh contour. Appendix B presents a direct perturbative calculation of equal-time correlation functions. Appendix C extends the results in the main body of the paper to interactions that do not conserve particle number.

2. Keldysh contour propagators

Consider the Hamiltonian of the standard real scalar field ϕ with a quartic interaction, in d spatial dimensions,

$$H = \int d^d x \left(\frac{1}{2} (\partial\phi)^2 + \frac{1}{2} m^2 \phi^2 + \frac{\lambda}{4!} \phi^4 \right). \quad (2.1)$$

It is convenient to switch to momentum space, writing the field in terms of creation and annihilation operators,¹

$$\phi(x) = \int \frac{d^d k}{\sqrt{2\omega_k}} \left(a_k e^{ik \cdot x} + a_k^\dagger e^{-ik \cdot x} \right). \quad (2.2)$$

Since we will be interested in the kinetic equation – which describes the rate of change of the occupation number – it is more natural to work with a_k instead of ϕ_k . In particular, our propagators and interactions will be expressed in terms of a_k and a_k^\dagger . Inserting ϕ into the Hamiltonian, the interaction has terms with varying numbers of creation and annihilation operators,

$$\int d^d x \phi(x)^4 = \int \prod_{i=1}^4 \frac{d^d k_i}{\sqrt{2\omega_{k_i}}} \left(6 a_{k_1}^\dagger a_{k_2}^\dagger a_{k_3} a_{k_4} \delta(\vec{k}_{12;34}) + (4 a_{k_1}^\dagger a_{k_2} a_{k_3} a_{k_4} \delta(\vec{k}_{1;234}) + a_{k_1} a_{k_2} a_{k_3} a_{k_4} \delta(\vec{k}_{1234}) + \text{h.c.}) \right) \quad (2.3)$$

where $\vec{k}_{12;34} \equiv \vec{k}_1 + \vec{k}_2 - \vec{k}_3 - \vec{k}_4$, $\vec{k}_{1;234} \equiv \vec{k}_1 - \vec{k}_2 - \vec{k}_3 - \vec{k}_4$ and $\vec{k}_{1234} \equiv \vec{k}_1 + \vec{k}_2 + \vec{k}_3 + \vec{k}_4$. The terms with different numbers of creation and annihilation operators appear separately in the tree-level kinetic equation. For simplicity, we will focus on the first term, which conserves particle number. The extension to the particle number nonconserving terms is straightforward, and is discussed in Appendix C at tree-level, and one-loop level for $\lambda\phi^4$ in Appendix C.1. However, the rules for evaluating a general loop diagram that we formulate Sec. 3.3 are natural specifically for a Hamiltonian with a definite number of creation and annihilation operators; for earlier studies for the full ϕ^3 and ϕ^4 interactions see [23–26].

Sticking to interactions that conserve particle number, we can just as well consider an arbitrary

¹In order to simplify notation, in this expression, and in all others, the factor of $(2\pi)^d$ is not explicitly written. In other words, in all momentum integrals one should replace $d^d k \rightarrow \frac{d^d k}{(2\pi)^d}$, and similarly for the momentum conserving delta function, $\delta(\vec{k}) \rightarrow (2\pi)^d \delta(\vec{k})$.

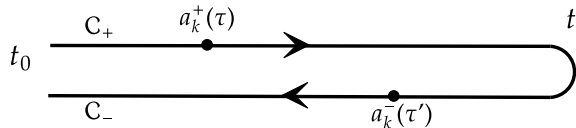


Figure 1: For a path integral to compute expectation values of operators at time t , time should run along the Keldysh contour, starting and ending at t_0 .

quartic interaction, $\lambda_{k_1 k_2 k_3 k_4} \equiv \lambda_{1234}$, that is some function of the momenta k_i ,

$$H = \int d^d k \omega_k a_k^\dagger a_k + \int \prod_{i=1}^4 d^d k_i \lambda_{k_1 k_2 k_3 k_4} a_{k_1}^\dagger a_{k_2}^\dagger a_{k_3} a_{k_4} \delta(\vec{k}_{12;34}) , \quad (2.4)$$

where $a_k(t)$ is the Fourier mode of the field and ω_k is the dispersion relation. We will assume that λ_{1234} is real, $\lambda_{1234} = \lambda_{3412}$; the results easily generalize to complex interactions. For the remainder of the main body of the paper, we work with the Hamiltonian (2.4). The equations of motion are, as usual, $\dot{a}_k = -i \frac{\partial H}{\partial a_k^\dagger}$, and the Lagrangian is,

$$L = -i \int d^d k \dot{a}_k^\dagger a_k - H . \quad (2.5)$$

We would like to compute expectation values of some operator $\mathcal{O}(t)$ in a given state. The path integral formalism naturally computes “in-out” correlation functions, in which operators are sandwiched between the state at time minus infinity and time plus infinity, rather than the in-in correlation functions that we need. The path integral is easily adopted to computing expectation values in a state by using a Keldysh (folded contour). Specifically,

$$\langle \mathcal{O}(t) \rangle = \int_{\mathcal{C}} D a_p D a_p^\dagger \mathcal{O}(t) e^{iS} , \quad (2.6)$$

where the contour \mathcal{C} runs from some initial time t_0 up to t , and then back to t_0 , see Fig. 1.

In Keldysh theory, see e.g. [27–29], it is common to double the number of fields, with one on the upper branch of the contour and one on the lower branch; this makes it easier to account for the contour being folded. We will call these a_k fields a_k^+ and a_k^- , where a_k^+ is on the upper branch (with time running the usual way) and a_k^- is on the lower branch, with time running backwards. We write

$$a_k(t) = a_k^+(t) + a_k^-(t) , \quad (2.7)$$

where a_k^+ is nonzero only on the upper branch and a_k^- is nonzero only on the lower branch. Since contour time runs backward along the lower branch, we pick up a minus sign from flipping time

in the integration measure, leading to the action:

$$S = \int dt \left[\int d^d k \left(i a_k^{+\dagger} \dot{a}_k^+ - i a_k^{-\dagger} \dot{a}_k^- \right) - H(a^+) + H(a^-) \right]. \quad (2.8)$$

As we will see in the next section, the propagator will mix the upper and lower branch fields due to the presence of time-derivative terms in the action.

Averaging over random forcing

Next, we introduce forcing and dissipation. This is an intermediate, technical step (both forcing and dissipation are set to zero at the end) that is a convenient way of placing the system in a particular state. Adding the forcing is straightforward, by linearly coupling the field to some forcing function f_k . Dissipation, on the other hand, cannot usually be accounted for in a classical action without introducing auxiliary degrees of freedom. In the Keldysh formalism, the required ‘‘auxiliary’’ degrees of freedom naturally appear, and we simply need to couple the fields on the upper and lower branch, see e.g. [30, 31],

$$S \rightarrow S + \int dt \int d^d k \left(i \gamma_k a_k^- a_k^{+\dagger} + i f_k^* (a_k^+ - a_k^-) \right) + \text{c.c.} . \quad (2.9)$$

With this choice of action, the equations of motion are:

$$\dot{a}_k^+ = -i \frac{\partial H(a^+)}{\partial a_k^{+\dagger}} - \gamma_k a_k^- + f_k \quad (2.10)$$

$$\dot{a}_k^- = -i \frac{\partial H(a^-)}{\partial a_k^{-\dagger}} - \gamma_k a_k^+ + f_k . \quad (2.11)$$

In the classical limit, the fields on the upper and lower branch become equal, $a_k^- = a_k^+$, and these are just the classical equations of motion in the presence of linearly coupled forcing and dissipation.

Like in the classical case, we will take the forcing to be Gaussian-random with variance F_k ,

$$P[f] \sim \exp \left(- \int dt \int d^d k \frac{|f_k(t)|^2}{F_k} \right), \quad \langle f_k(t) f_p^*(t') \rangle = F_k \delta(\vec{k} - \vec{p}) \delta(t - t'). \quad (2.12)$$

Integrating out the forcing leaves us with the action,

$$S = \int dt \left[\int d^d k i \left((a_k^{+\dagger} \dot{a}_k^+ - a_k^{-\dagger} \dot{a}_k^-) + \gamma_k (a_k^{+\dagger} a_k^- - a_k^{-\dagger} a_k^+) + F_k |a_k^+ - a_k^-|^2 \right) - H(a^+) + H(a^-) \right]. \quad (2.13)$$

It is useful to work with fields that are the sum and difference of the fields on the upper and lower branches,

$$A_k = \frac{1}{\sqrt{2}} (a_k^+ + a_k^-), \quad \eta_k = \frac{1}{\sqrt{2}} (a_k^+ - a_k^-). \quad (2.14)$$

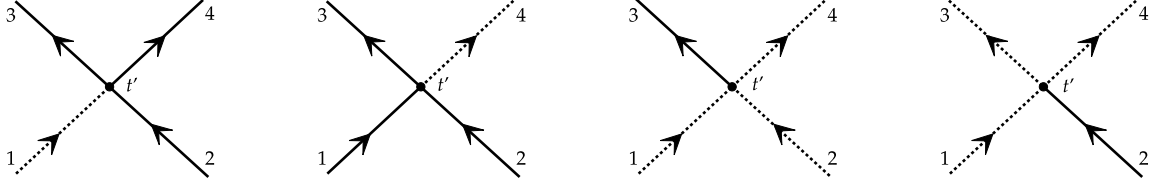


Figure 2: The first two vertices, which have one η field and three A fields, are classical. The last two vertices, which have one A field and three η fields, are quantum.

where we use the shorthand $t_{12} \equiv t_1 - t_2$. As is now clear, G^K is the Keldysh Green's function, while G^R and G^A are the retarded and advanced Green's functions, respectively. The occupation number $n_k = \langle a_k^\dagger(t)a_k(t) \rangle$ of mode k can be expressed in terms of the three Green's functions at equal time (see Appendix A),

$$n_k = \lim_{t_2 \rightarrow t_1} \frac{1}{2} \left[G_k^K(t_1, t_2) + G_k^A(t_1, t_2) - G_k^R(t_1, t_2) \right] = \frac{F_k}{2\gamma_k} - \frac{1}{2}. \quad (2.22)$$

We will be taking both F_k and γ_k to zero, $F_k, \gamma_k \rightarrow 0$, while maintaining constant n_k . In this limit we may simplify the Keldysh Green's function (2.19),

$$G_{k,\omega}^K = (2n_k + 1)\delta(\omega - \omega_k), \quad G_k^K(t_1, t_2) = (2n_k + 1)e^{-i\omega_k t_{12}}. \quad (2.23)$$

Turning to the interacting part of the Lagrangian (2.15), there are four types of vertices, represented by the Feynman diagrams shown in Fig. 2. The Feynman rule is to simply assign a value of $-i\lambda_{3412}$.

Averaging over initial conditions

From looking at the form of the retarded (2.20) and Keldysh (2.23) Green's functions, it is clear that we could have obtained the same result without ever introducing forcing and dissipation, by instead simply picking an appropriate Gaussian initial state. In particular, in the absence of forcing and dissipation, the free part of the action takes the form L_{free} in (2.15) with $F_k = \gamma_k = 0$,

$$S_{\text{free}} = i \int d^d k \int dt_1 dt_2 \begin{pmatrix} A_k^\dagger(t_1) & \eta_k^\dagger(t_1) \end{pmatrix} \widehat{\Sigma}_k(t_1, t_2) \begin{pmatrix} A_k(t_2) \\ \eta_k(t_2) \end{pmatrix} \quad (2.24)$$

where

$$\widehat{\Sigma}_k(t_1, t_2) = \begin{pmatrix} 0 & (\partial_{t_1} + i\omega_k)\delta(t_1 - t_2) \\ (\partial_{t_1} + i\omega_k)\delta(t_1 - t_2) & 0 \end{pmatrix}. \quad (2.25)$$

The Green's function is given by the inverse, $\widehat{G}_k \widehat{\Sigma}_k = \mathbb{1}$. In terms of

$$\widehat{G}_k(t_1, t_2) = \begin{pmatrix} G_k^K(t_1, t_2) & G_k^R(t_1, t_2) \\ G_k^A(t_1, t_2) & 0 \end{pmatrix} \quad (2.26)$$

we see that G^R and G^K satisfy,

$$-\partial_{t_2} G_k^{R,A}(t_1, t_2) + i\omega_k G_k^{R,A}(t_1, t_2) = \delta(t_1 - t_2) , \quad (2.27)$$

$$-\partial_{t_2} G_k^K(t_1, t_2) + i\omega_k G_k^K(t_1, t_2) = 0 , \quad (2.28)$$

which means that G^R is given by (2.20), while G^K takes the form,

$$G_k^K(t_1, t_2) = g_k e^{-i\omega_k t_{12}} \quad (2.29)$$

with arbitrary g_k . In the path integral (2.6), the precise Gaussian initial state at time t_0 can be incorporated through the choice of boundary conditions for $G_k(t_1, t_2)$ when $t_1=t_2=t_0$, see e.g. [38]. The choice $g_k = 2n_k + 1$ ensures that (2.29) matches (2.23).

While for a free theory one can pick any value of n_k , for an interacting theory the choice is strongly constrained. In particular, our derivation of the kinetic equation will assume that the state is close to stationary. One option is that the state is close to thermal. However, this is not the only option: for the (stationary) finite-flux solutions, upon obtaining the kinetic equation, as we will do in the next section, one finds the n_k so that the collision term in the kinetic equation vanishes. In this sense, n_k is determined a posteriori.

3. Correlation functions and the kinetic equation

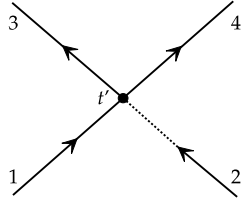
The kinetic equation encodes the dynamics, describing how the occupation number of mode k evolves over time. As shown in Appendix A, this can be expressed in terms of the imaginary part of the equal-time four-point function,

$$\frac{\partial n_1}{\partial t} = 4 \operatorname{Im} \int \prod_{i=2}^4 d^d k_i \delta(\vec{k}_{12;34}) \lambda_{1234} \langle a_1^\dagger a_2^\dagger a_3 a_4 \rangle(t) = \operatorname{Im} \int \prod_{i=2}^4 d^d k_i \delta(\vec{k}_{12;34}) \lambda_{1234} \langle A_1^\dagger A_2^\dagger A_3 A_4 \rangle(t) \quad (3.1)$$

Here, the creation and annihilation operators in the middle expression belong to the original theory (2.4), whereas the last correlation function is on the Keldysh contour and the A 's represent the Keldysh-rotated classical fields (2.14).

3.1. Tree-level kinetic equation

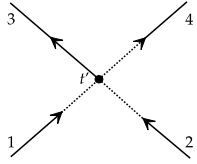
In this section, we compute the equal-time four-point function $\langle A_1^\dagger A_2^\dagger A_3 A_4 \rangle(t)$ to leading order in the coupling, thereby reproducing the standard quantum kinetic equation. At tree level, each contributing diagram contains a single vertex. One type of diagram involves three classical fields (A) and one quantum field (η) at the vertex, which we refer to as a classical vertex. For instance,



$$\begin{aligned}
 &= -2i\lambda_{3412} \int dt' G_{k_1}^K(t', t) G_{k_2}^A(t', t) G_{k_3}^K(t, t') G_{k_4}^K(t, t') \\
 &= 2\lambda_{3412} (2n_1+1)(2n_3+1)(2n_4+1) \frac{1}{\omega_{34;12} - i\epsilon} . \tag{3.2}
 \end{aligned}$$

The three other diagrams of this type immediately follow by choosing one of the other three legs attached to the vertex to be the η field, denoted by the dashed line.

Another type of diagram involves three quantum and one classical field at the vertex, which we refer to as a quantum vertex. For instance,



$$= -2i\lambda_{3412} \int dt' G_{k_1}^A(t', t) G_{k_2}^A(t', t) G_{k_3}^K(t, t') G_{k_4}^R(t, t') = -2\lambda_{3412} \frac{(2n_3+1)}{\omega_{34;12} - i\epsilon} . \tag{3.3}$$

Similarly, three additional diagrams can be obtained by assigning one of the other legs to be the classical field, represented by the solid line. By summing all eight diagrams (four classical and four quantum) we obtain:

$$\langle A_1^\dagger A_2^\dagger A_3 A_4(t) \rangle_{\text{tree}} = 16\lambda_{3412} \left((n_1+1)(n_2+1)n_3n_4 - n_1n_2(n_3+1)(n_4+1) \right) \frac{1}{\omega_{34;12} - i\epsilon} . \tag{3.4}$$

Explicitly, we used that,

$$N_1 N_2 N_3 N_4 \left(\frac{1}{N_1} + \frac{1}{N_2} - \frac{1}{N_3} - \frac{1}{N_4} \right) + (N_1 + N_2 - N_3 - N_4) = 8 \left((n_1+1)(n_2+1)n_3n_4 - n_1n_2(n_3+1)(n_4+1) \right) , \tag{3.5}$$

where $N_i \equiv 2n_i + 1$ and on the left-hand side the first term is from the classical vertices and the second term is from the quantum vertices. Using (3.1), we obtain the tree-level kinetic equation,

$$\frac{\partial n_1(t)}{\partial t} = 16\pi \int \prod_{i=2}^4 d^d k_i |\lambda_{1234}|^2 \left((n_1+1)(n_2+1)n_3n_4 - n_1n_2(n_3+1)(n_4+1) \right) \delta(\omega_{12;34}) \delta(\vec{k}_{12;34}) . \tag{3.6}$$

This is simply the standard quantum Boltzmann equation, where the scattering cross-section is the one at weak coupling. In the highly quantum regime $n_k \ll 1$ this becomes the classical Boltzmann equation for particles, whereas in the high occupation number $n_k \gg 1$ regime it becomes the classical kinetic equation for waves.

Returning to the integral appearing in (3.2), we can explicitly see the difference between the two types of averaging under consideration. The first, involving Gaussian random forcing and dissipation, means that the integral takes the form,

$$\int_{t_0}^t dt' e^{-i(\omega_{34;12}-i\epsilon)(t-t')} = \frac{-i}{\omega_{34;12}-i\epsilon}, \quad (3.7)$$

As a result of $\epsilon > 0$, the contribution from the initial time t_0 doesn't enter. On the other hand, when averaging over a Gaussian initial state, there is no dissipation, so the expression instead takes the form,

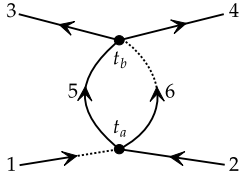
$$\begin{aligned} \int_{t_0}^t dt' e^{-i\omega_{34;12}(t-t')} &= \frac{1 - e^{-i\omega_{34;12}(t-t_0)}}{i\omega_{34;12}} = -i \frac{1 - \cos \omega_{34;12}(t-t_0)}{\omega_{34;12}} + \frac{\sin \omega_{34;12}(t-t_0)}{\omega_{34;12}} \\ &\rightarrow \frac{-i}{\omega_{34;12}} + \pi \delta(\omega_{34;12}), \quad \text{for } t-t_0 \rightarrow \infty. \end{aligned} \quad (3.8)$$

In the second line, we took the late-time limit. In the imaginary component, the cosine oscillates rapidly and can therefore be dropped when integrated against a smooth function of time. The real part becomes a delta function, since, if $\omega_{34;12}$ is not small, the numerator oscillates rapidly at late times and the expression vanishes, in the same sense. In short, whether averaging over Gaussian-random forcing and dissipation (with the variance of the former and the magnitude of the latter taken to zero) or over Gaussian initial conditions, the result is the same at late times.

3.2. One-loop-level kinetic equation

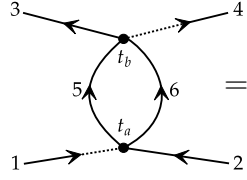
We now look at the one-loop contributions to the equal-time four-point function, $\langle A_1^\dagger A_2^\dagger A_3 A_4 \rangle$. Topologically, there is a single diagram, shown below. However, since we have two fields (A and η), there are multiple variations of this diagram, depending on whether the propagators are Keldysh, retarded, or advanced. We begin with the s -channel diagrams.

A diagram with two classical vertices is,



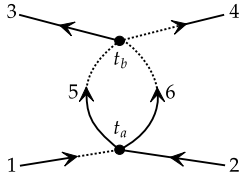
$$\begin{aligned}
&= - \int d^d k_5 d^d k_6 \delta(\vec{k}_{12;56}) \lambda_{3456} \lambda_{5612} \int dt_a dt_b G_{k_1}^A(t_a, t) G_{k_2}^K(t_a, t) G_{k_5}^K(t_b, t_a) G_{k_6}^A(t_b, t_a) G_{k_3}^K(t, t_b) G_{k_4}^K(t, t_b) \\
&= \frac{(2n_1 + 1)(2n_3 + 1)(2n_4 + 1)}{\omega_{34;12} - i\epsilon} \int d^d k_5 d^d k_6 \delta(\vec{k}_{12;56}) \lambda_{3456} \lambda_{5612} \frac{(2n_5 + 1)}{\omega_{34;56} - i\epsilon}. \tag{3.9}
\end{aligned}$$

where, in the second equality, we have evaluated the time integrals, whose structure is identical to the classical case [17]. Another diagram with two classical vertices is,



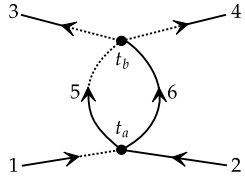
$$\begin{aligned}
&= - \frac{(2n_2 + 1)(2n_3 + 1)}{\omega_{34;12} - i\epsilon} \int d^d k_5 d^d k_6 \delta(\vec{k}_{12;56}) \lambda_{3456} \lambda_{5612} (2n_5 + 1)(2n_6 + 1) \\
&\quad \left[\frac{1}{\omega_{56;12} - i\epsilon} + \frac{1}{\omega_{34;56} - i\epsilon} \right] \tag{3.10}
\end{aligned}$$

There are also diagrams with one classical and one quantum vertex, such as,



$$= - \frac{(2n_2 + 1)(2n_3 + 1)}{\omega_{34;12} - i\epsilon} \int d^d k_5 d^d k_6 \delta(\vec{k}_{12;56}) \lambda_{3456} \lambda_{5612} \frac{1}{\omega_{34;56} - i\epsilon}. \tag{3.11}$$

and



$$= \frac{2n_4 + 1}{\omega_{34;12} - i\epsilon} \int d^d k_5 d^d k_6 \delta(\vec{k}_{12;56}) \lambda_{3456} \lambda_{5612} \frac{2n_6 + 1}{\omega_{34;56} - i\epsilon}. \tag{3.12}$$

All other diagrams can be derived from these four by exchanging the mode variables, and potentially complex conjugating. Note that a one-loop diagram involving two quantum vertices vanishes identically: the presence of two quantum vertices forces the loop into one of the following

two structures,

$$\begin{aligned}
 \text{Diagram 1} &= G_{k_5}^R(t_b, t_a) G_{k_6}^A(t_b, t_a) \\
 \text{Diagram 2} &= G_{k_5}^R(t_b, t_a) G_{k_6}^R(t_a, t_b) \quad (3.13)
 \end{aligned}$$

both of which have conflicting time-orderings of t_a and t_b , $\theta(t_{ab})\theta(-t_{ab})$, forcing the integral to vanish.

Summing over the diagrams, the total s -channel contribution to the equal-time four-point function is

$$\begin{aligned}
 \langle A_1^\dagger A_2^\dagger A_3 A_4 \rangle_{s\text{-channel}} &= \frac{16}{\omega_{34;12} - i\epsilon} \int d^d k_5 d^d k_6 \lambda_{3456} \lambda_{5612} \left[(n_3 + n_4 + 1) \frac{n_1 n_2 (n_5 + n_6 + 1) - n_5 n_6 (n_1 + n_2 + 1)}{\omega_{56;12} - i\epsilon} \right. \\
 &\quad \left. + (n_1 + n_2 + 1) \frac{n_3 n_4 (n_5 + n_6 + 1) - n_5 n_6 (n_3 + n_4 + 1)}{\omega_{34;56} - i\epsilon} \right] \delta(\vec{k}_{12;56}) \quad (3.14)
 \end{aligned}$$

We also need to look at the one-loop diagrams in the t -channel. An example is

$$\text{Diagram (3.15)} \quad (3.15)$$

where momentum conservation imposes $k_3 + k_5 = k_1 + k_6$. There are other t -channel diagrams with possible classical and quantum vertices, similar to those in the s -channel. It is simple to obtain the t -channel contribution from the s -channel result by a symmetry transformation [16], sending $6 \rightarrow -6$, $3 \leftrightarrow -2$. This transforms the coupling $\lambda_{5612} \rightarrow \lambda_{5-61-3} \equiv \lambda_{3516}$, whereas for the occupation numbers $i \rightarrow -i$ sends $n_i \rightarrow -1 - n_i$, and there is an overall sign of -1 for each arrow that is flipped (3 in this case). Accounting for the extra combinatorial factor of 2, we get that the t -channel contribution is

$$\begin{aligned}
 \langle A_1^\dagger A_2^\dagger A_3 A_4 \rangle_{t\text{-channel}} &= \frac{32}{\omega_{34;12} - i\epsilon} \int d^d k_5 d^d k_6 \lambda_{3516} \lambda_{4625} \left[(n_2 - n_4) \frac{n_1 n_6 (n_3 + n_5 + 1) - n_3 n_5 (n_1 + n_6 + 1)}{\omega_{35;16} - i\epsilon} \right. \\
 &\quad \left. + (n_1 - n_3) \frac{n_2 n_5 (n_4 + n_6 + 1) - n_4 n_6 (n_2 + n_5 + 1)}{\omega_{46;25} - i\epsilon} \right] \delta(\vec{k}_{16;35}) \quad (3.16)
 \end{aligned}$$

The u -channel follows trivially by exchanging 3 and 4 in the t -channel contribution.

Thus, the quantum kinetic equation to order λ^3 is, via (3.1), expressed in terms of the equal-

time four-point function, which is the sum of the tree-level and one-loop diagrams,

$$\frac{\partial n_1}{\partial t} = 16\pi \int \prod_{i=2}^4 d^d k_i \lambda_{1234}^2 \left((n_1+1)(n_2+1)n_3n_4 - n_1n_2(n_3+1)(n_4+1) \right) \left(1 + 2\mathcal{L}_+ + 8\mathcal{L}_- \right) \delta(\omega_{12;34}) \delta(\vec{k}_{12;34}) . \quad (3.17)$$

where

$$\mathcal{L}_+ = 2 \int d^d k_5 d^d k_6 \frac{\lambda_{5612} \lambda_{3456}}{\lambda_{1234}} \frac{n_5 + n_6 + 1}{\omega_{12;56}} \delta(\vec{k}_{12;56}) , \quad \mathcal{L}_- = 2 \int d^d k_5 d^d k_6 \frac{\lambda_{3516} \lambda_{4625}}{\lambda_{1234}} \frac{n_6 - n_5}{\omega_{16;35}} \delta(\vec{k}_{16;35}) . \quad (3.18)$$

Here, the $1/\omega$ denominators are understood as their principal values. The s -channel one-loop four-point function gives the \mathcal{L}_+ term, while the t and u channels each give an \mathcal{L}_- term. In addition, here ω_k is really the one-loop renormalized frequency,

$$\omega_1 \rightarrow \omega_1 + 4 \int d^d k_2 \lambda_{1212} \left(n_2 + \frac{1}{2} \right) . \quad (3.19)$$

3.3. Higher loop diagrams

In this section, we provide a simple prescription for determining the contribution of any Feynman diagram to an equal-time correlation function. This serves as a quantum generalization of the rules presented in [17].

When evaluating a given Feynman diagram, it is useful to choose a definite time ordering of the internal vertices. Once this is done, the time-dependent portion of the integrand is simply a product of exponentials $e^{-i\omega_k t_{ab}}$ which connect vertices at times t_a and t_b ; the Keldysh, retarded, and advanced Green's function all have this same dependence, (2.19– 2.21). The result of the time integrals will be identical to that discussed in [17]. Specifically, one moves from the earliest time to the latest time.³ At each step, one draws an imaginary loop enclosing all previously visited vertices and writes down a factor

$$\frac{1}{\omega_i + \omega_j + \dots - \omega_a - \omega_b - \dots - i\epsilon} , \quad (3.20)$$

where $\omega_i, \omega_j, \dots$ are the frequencies of all lines leaving this imaginary loop and $\omega_a, \omega_b, \dots$ are the frequencies of all lines entering the imaginary loop. For example, for the s -channel diagram in the previous section, such as the one in (3.9), the time ordering $t_a > t_b$ yields the factor,

$$\frac{1}{\omega_{34;56} - i\epsilon} \frac{1}{\omega_{34;12} - i\epsilon} \quad (3.21)$$

³We are using an opposite time ordering convention from [17].

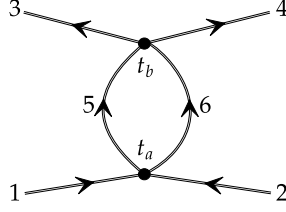


Figure 3: The double line on the propagator indicates that it can be either a Keldysh Green’s function (solid single line), or a retarded or advanced Green’s function (solid/dashed line). This figure therefore includes all the s -channel diagrams, shown earlier in Figs. 3.9 – 3.12.

where the first term comes from the first imaginary loop, enclosing vertex b , and the second term comes from the imaginary loop enclosing both vertices. This matches the ω dependence written in (3.9), (3.11), (3.12), which, due to the advanced Green’s function within the loop, must follow this time ordering. One of the pieces in (3.10)– which, as a result of both Green’s functions within the loop being Keldysh – can have either ordering, $t_b > t_a$ or $t_b < t_a$. In fact, rule (3.20) becomes evident when computing the expectation value directly in quantum mechanical perturbation theory, see Appendix B. In particular, as one evolves the state from t_0 to t , each intermediate interaction vertex modifies the energy, by creating and annihilating particles. These ω denominator factors reflect the total energy (in the free theory) at these intermediate times between t_0 and t .

In the previous section, for each vertex we had a choice of if it is a classical or a quantum vertex. In fact, we can consider all the choices simultaneously. Let us redraw the s -channel diagram in (3.9), being agnostic if each vertex is classical or quantum, and correspondingly if the propagators are Kelydsh, retarded, or advanced, see Fig. 3. Now consider the time ordering $t_a > t_b$. We look at vertex a , and see that we cannot have a dashed line coming out from a in the direction of b . Since there are two lines going from a to b , this means the vertex at a must be classical, and that the one dashed line coming out of the classical vertex must be going in the direction of the external time. The other line going to the external time must therefore be the Keldysh propagator, so we get a factor of n_1+n_2 . Moving now to vertex b , any of the lines coming out of it can be dashed or solid, so the vertex can be either classical or quantum. In total we get the factor,

$$\begin{aligned} (N_1+N_2) \left[N_3 N_4 N_5 N_6 \left(\frac{1}{N_5} + \frac{1}{N_6} - \frac{1}{N_3} - \frac{1}{N_4} \right) + (N_5+N_6-N_3-N_4) \right] \\ = 16(n_1+n_2+1) \left(n_3 n_4 (n_5+1)(n_6+1) - (n_3+1)(n_4+1)n_5 n_6 \right) \end{aligned} \quad (3.22)$$

where $N_i \equiv 2n_i + 1$, see (3.5). Combining (3.21) with (3.22), and the appropriate combinatorial factor and multiplying by the couplings, reproduces the second term in (3.14).

The other option for the time ordering of the internal vertices is $t_a < t_b$. From the time

integral we get the factor,

$$\frac{1}{\omega_{56;12}-i\epsilon} \frac{1}{\omega_{34;12}-i\epsilon} \quad (3.23)$$

where the first term comes from the first imaginary loop, enclosing vertex at a , and the second term comes from the imaginary loop enclosing both vertices. The factor involving the occupation numbers is,

$$\begin{aligned} - (N_3+N_4) \left[N_1 N_2 N_5 N_6 \left(\frac{1}{N_1} + \frac{1}{N_2} - \frac{1}{N_5} - \frac{1}{N_6} \right) + (N_1+N_2-N_5-N_6) \right] \\ = -16(n_3+n_4+1) \left((n_1+n_2+1)n_5 n_6 - (n_5+n_6+1)n_1 n_2 \right) \end{aligned} \quad (3.24)$$

where the first term, N_3+N_4 , comes from vertex b having to be classical. Combining (3.23) and (3.24) gives the first term in (3.14).

We are now ready to give simple rules for writing down any equal-time correlation function to any order in the coupling. For a given Feynman diagram (drawn for the theory expressed in terms of the original variables – only a fields):

Rules:

1. Pick an ordering of the times at each vertex. The time t at which the correlation function is being evaluated must be the largest time.
2. Start at the earliest time on the diagram and move from vertex to vertex in increasing order of their times, until finally reaching the vertex at the latest time. Each subsequent vertex must be adjacent to at least one previously visited vertex. At each step in this process, draw an imaginary loop enclosing all vertices visited so far. Write down a factor of

$$\frac{1}{\omega_i+\omega_j+\dots-\omega_a-\omega_b-\dots-i\epsilon} \quad (3.25)$$

where $\omega_i, \omega_j, \dots$ are the frequencies of all lines leaving this imaginary loop and $\omega_a, \omega_b, \dots$ are the frequencies of all lines entering the imaginary loop.

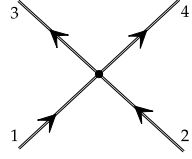
3. Start at the latest time on the diagram and move from vertex to vertex in decreasing order of their times, until finally reaching the vertex at the earliest time. Each next vertex must be a neighbor of at least one previously visited vertex. At each step, when writing down the occupation number factor for each vertex only look at the lines coming out of the vertex that are going to another vertex that is at a later time. This makes the interaction at this vertex effectively q body, if there are q such lines. Let a be the index for the lines entering the effective vertex and i the index for the lines leaving the effective vertex. Write down a

factor of

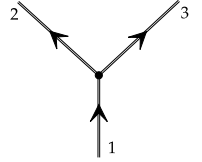
$$\prod_a n_a \prod_i (1 + n_i) - \prod_a (1 + n_a) \prod_i n_i \quad (3.26)$$

This is the standard result that one expects for a tree-level interaction: it is weighted by the product of the occupation numbers n of the ingoing particles, and by a factor of the product of $1 + n$ for the outgoing particles (reflecting the Bose enhancement). If we had fermions instead of bosons we would simply replace this by $1 - n$. The second term is the time reverse process.


Explicitly, for quartic, cubic, quadratic, and one-body effective interactions this factor is:



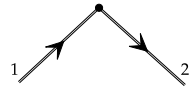
$$= n_1 n_2 (1 + n_3)(1 + n_4) - n_3 n_4 (1 + n_1)(1 + n_2) \quad (3.27)$$



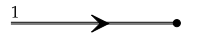
$$= n_1 (1 + n_2)(1 + n_3) - (1 + n_1) n_2 n_3 \quad (3.28)$$



$$= n_1 n_2 - (1 + n_1)(1 + n_2) = -(1 + n_1 + n_2) \quad (3.29)$$



$$= n_1 (1 + n_2) - (1 + n_1) n_2 = n_1 - n_2 \quad (3.30)$$



$$= n_1 - (1 + n_1) = -1 \quad (3.31)$$

4. Multiply the result by the product of the couplings at each vertex, and integrate the resulting expression over all internal momenta.
5. Repeat Steps 1 through 5 for all possible time orderings, sum the results, and include the appropriate Feynman diagram combinatorics factor.

Examples

Let us see how Step 3 reproduces (3.24), which was found for the s -channel one loop diagram in Fig. 3. For $t_a > t_b$, we begin at the vertex at t_a . We have an effective 2-body vertex, since we only look at the lines going to the external time. From the form in (3.29) this gives the factor $-(1 + n_1 + n_2)$. Now, examining the b vertex, since it is at the earliest time, it is an effective 4-body

vertex. From the form in (3.27) this gives the factor $n_5 n_6 (1+n_3)(1+n_4) - (1+n_5)(1+n_6)n_3 n_4$.

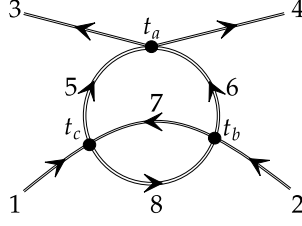


Figure 4: A two-loop diagram.

Let us now give some examples of applying these rules to higher-loop diagrams. For instance, consider the two-loop diagram shown in Fig. 4. The time ordering $t_a > t_b > t_c$ gives the factor,

$$\frac{1}{\omega_{58;17}-i\epsilon} \frac{1}{\omega_{56;12}-i\epsilon} \frac{1}{\omega_{34;12}-i\epsilon} (n_3+n_4+1)(n_2-n_6) \left(n_1 n_7 (n_5+1)(n_8+1) - (n_1+1)(n_7+1)n_5 n_8 \right) \quad (3.32)$$

On the other hand, the ordering $t_c > t_b > t_a$ gives the factor,

$$\frac{\left(n_2 n_8 (n_7+1) - (n_2+1)(n_8+1)n_7 \right) \left(n_5 n_6 (n_3+1)(n_4+1) - (n_5+1)(n_6+1)n_3 n_4 \right)}{(\omega_{34;56}-i\epsilon)(\omega_{347;258}-i\epsilon)(\omega_{34;12}-i\epsilon)}. \quad (3.33)$$

There are four additional time orderings to consider, but we stop here.

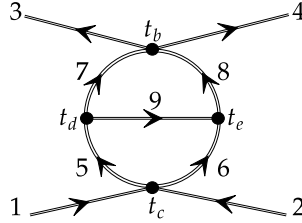


Figure 5: A two-loop diagram in a theory with both cubic and quartic interactions.

These rules are not specific to quartic interactions. For instance, consider the diagram in Fig. 5, taken from Fig. 6 of [17], in a theory with both quartic and cubic interactions. An example of a time ordering is $t_b > t_e > t_c > t_d$, which gives the factor,

$$\frac{(n_3+n_4+1) \left(n_1 n_2 (n_6+1) - (n_1+1)(n_2+1)n_6 \right) \left(n_5 (n_7+1)(n_9+1) - (n_5+1)n_7 n_9 \right)}{(\omega_{79;5}-i\epsilon)(\omega_{679;12}-i\epsilon)(\omega_{78;12}-i\epsilon)(\omega_{34;12}-i\epsilon)} \quad (3.34)$$

Setting up the calculation of the correlation functions in standard quantum mechanical perturbation theory, as done in Appendix B, shows that for each diagram, every term contains either an n_i or a $(1+n_i)$ factor for each momentum p_i appearing in the diagram. This is just because either

the annihilation operator acts first followed by the action of the creation operator, $a_i^\dagger a_i |n_i\rangle = n_i |n_i\rangle$, or vice-versa, $a_i a_i^\dagger |n_i\rangle = (n_i + 1) |n_i\rangle$. The power of (3.26) is that it accounts for minus signs, telling us how all these terms combine.

4. Discussion

The Boltzmann equation describes the rate of change of particle number, accounting for the two-to-two scattering amplitude while neglecting all other multi-particle scattering processes. As the density increases, it stops being legitimate to ignore such terms. Assuming weak coupling and a state that is nearly homogenous and stationary, we have explicitly computed the next-order terms in the density, and provided a simple algorithm for writing down terms at any order.

We have worked within the context of quantum field theory, which describes both particles and waves. Classically, the kinetics of waves and particles have qualitatively different structures. The first-principles description of the kinetics of classical particles is through the celebrated BBGKY hierarchy, which relates the rate of change of a one-particle distribution to a two-particle distribution, whose rate of change is, in turn, expressed in terms of a three-particle distribution, and so on. A low density, combined with the assumption of chaos, allows one to truncate the hierarchy by factorizing the two-particle distribution into a product of two one-particle distributions, yielding the Boltzmann equation. The kinetics of classical waves, on the other hand, relates the rate of change of an equal-time two-point correlation function to a four-point correlation function via the equations of motion, whose rate of change is, in turn, expressed in terms of a six-point function, and so forth. Weak interactions, and a state that is nearly Gaussian, allows one to factorize higher-point functions into two-point functions – occupation numbers. It may be useful to study the classical particle limit of our results for the higher-order kinetic equation for quantum fields.

The wave kinetic equation has been of particular interest recently due to the existence of stationary, far-from-equilibrium, scale-invariant constant-flux solutions, $n_k \sim k^{-\gamma}$, which appear in a broad range of physical contexts with weakly interacting solutions, such as: gravity waves in the ocean [39, 40] and capillary waves [41, 42], Bose gases [43–49], and cascades in early universe reheating [50, 51] and following hadron collisions [52]. Generally, the classical wave limit ($n_k \gg 1$) is taken, in order to have scale-invariant behavior. Nevertheless, through use of (3.1), one can search for stationary far-from-equilibrium states in any quantum field theory in which the four-point function can be computed; the prime example so far has been large- N theories [53–56].

Acknowledgments

We thank I. Rothstein, D. Schubring, and M. Smolkin for helpful discussions. XYH is supported by the Shuimu Tsinghua Scholar Program at Tsinghua University and a fellowship from the China Postdoctoral Science Foundation (Certificate No. 2024M761598). VR is supported by

NSF grant 2209116 and by BSF grant 2022113. XYH thanks the NYU Center for Cosmology and Particle Physics and the CUNY Graduate Center for their hospitality, during which part of this work was carried out.

A. Contour-ordered propagators

In this appendix, we review the basics of contour-ordered Green's functions and their relation to the occupation number of a given mode.

The contour-ordered Green's function $G_{\mathcal{C}}(\tau, \tau') \equiv \langle T_{\mathcal{C}}\{a(\tau)a^\dagger(\tau')\} \rangle$ is defined as

$$G_{\mathcal{C}}(\tau, \tau') = \begin{cases} G^{++}(\tau, \tau') \equiv \langle T_{\mathcal{C}}\{a^+(\tau)a^{+\dagger}(\tau')\} \rangle = G^T(t, t') = \langle T\{a(t)a^\dagger(t')\} \rangle, & \tau, \tau' \in \mathcal{C}_+, \\ G^{+-}(\tau, \tau') \equiv \langle a^{-\dagger}(\tau')a^+(\tau) \rangle = G^<(t, t') = \langle a^\dagger(t')a(t) \rangle, & \tau \in \mathcal{C}_+, \tau' \in \mathcal{C}_- \\ G^{-+}(\tau, \tau') \equiv \langle a^-(\tau)a^{+\dagger}(\tau') \rangle = G^>(t, t') = \langle a(t)a^\dagger(t') \rangle, & \tau \in \mathcal{C}_-, \tau' \in \mathcal{C}_+ \\ G^{--}(\tau, \tau') \equiv \langle T_{\mathcal{C}}\{a^-(\tau)a^{-\dagger}(\tau')\} \rangle = G^{\bar{T}}(t, t') = \langle \bar{T}\{a(t)a^\dagger(t')\} \rangle, & \tau, \tau' \in \mathcal{C}_-, \end{cases} \quad (\text{A.1})$$

where a^\dagger and a are the creation and annihilation operators in the original theory (2.4) and the Schwinger-Keldysh contour is defined as $\mathcal{C} = \mathcal{C}_+ \cup \mathcal{C}_-$, t and t' represent the values of τ and τ' , respectively, regardless of whether they are on the \mathcal{C}_+ or \mathcal{C}_- branch, see Fig. 1. For example, we have the operator relation $a(t) = a^+(t) = a^-(t)$. The symbol T denotes the time-ordering operator, whereas the \bar{T} represents the anti-time-ordering operator. Here, $\langle \mathcal{O} \rangle$ represents the transition amplitude from the initial state $|\Omega\rangle$ at $t = t_0$ back to itself, with an operator (in the Heisenberg or interaction picture) inserted somewhere on the contour, $\langle \mathcal{O} \rangle \equiv \langle \Omega | \mathcal{O} | \Omega \rangle$.

The contour-ordered Green's function can naturally be organized into a two-by-two matrix form in the (a^+, a^-) basis,

$$G_{\mathcal{C}} = \begin{pmatrix} G^{++} & G^{+-} \\ G^{-+} & G^{--} \end{pmatrix} = \begin{pmatrix} G^T & G^< \\ G^> & G^{\bar{T}} \end{pmatrix}. \quad (\text{A.2})$$

By performing the Keldysh rotation (2.14), we obtain the matrix in the (A, η) basis,

$$G_{\mathcal{C}} = \begin{pmatrix} G^K & G^R \\ G^A & 0 \end{pmatrix} \quad (\text{A.3})$$

where

$$G^K = G^> + G^< = G^T + G^{\bar{T}}, \quad (\text{A.4})$$

$$G^R = G^T - G^< = G^> - G^{\bar{T}}, \quad (\text{A.5})$$

$$G^A = G^T - G^> = G^< - G^{\bar{T}}. \quad (\text{A.6})$$

The superscripts K , R , and A denote the Keldysh, retarded, and advanced Green's functions, respectively. By substituting (A.1) into (A.4) – (A.6), one gets

$$G^K(t, t') = \langle \{a^\dagger(t'), a(t)\} \rangle, \quad G^R(t, t') = \langle [a(t), a^\dagger(t')] \rangle \theta(t-t'), \quad G^A(t, t') = \langle [a^\dagger(t'), a(t)] \rangle \theta(t'-t). \quad (\text{A.7})$$

The time ordering of these Green's functions is now explicitly defined. It is straightforward to verify that the expressions in (2.16) – (2.18) match those in (A.7).

As indicated by (A.1), the occupation number $n \equiv \langle a^\dagger(t)a(t) \rangle$ is given by $G^<(t, t')$ in the limit $t' \rightarrow t$. Using the relations (A.4)–(A.6), we express the occupation number in terms of G^K , G^A and G^R as

$$n = \lim_{t' \rightarrow t} G^<(t, t') = \lim_{t' \rightarrow t} \frac{1}{2} \left[G^K(t, t') + G^A(t, t') - G^R(t, t') \right]. \quad (\text{A.8})$$

Kinetic equation and equal-time four-point function

Here, we derive the quantum kinetic equation (3.1), which relates the change in the occupation number to an equal-time four-point function.

Combining the Heisenberg equation of motion for the Hamiltonian (2.4),

$$\dot{a}_k = i[H, a_k] = -i\omega_k a_k - 2i \int \prod_{i=2}^4 d^d k_i \lambda_{k234} a_2^\dagger a_3 a_4, \quad (\text{A.9})$$

with its Hermitian conjugate, we obtain the time derivative of the occupation number of mode k , $n_k \equiv \langle a_k^\dagger(t)a_k(t) \rangle$,

$$\frac{\partial n_k}{\partial t} = \langle \dot{a}_k^\dagger a_k \rangle + \langle a_k^\dagger \dot{a}_k \rangle = 2i \int \prod_{i=2}^4 d^d k_i \left(\lambda_{k234}^* \langle a_4^\dagger a_3^\dagger a_2 a_k \rangle - \lambda_{k234} \langle a_k^\dagger a_2^\dagger a_3 a_4 \rangle \right). \quad (\text{A.10})$$

where we used that $[a_i, a_j^\dagger] = \delta_{ij}$. For an operator \mathcal{O} and two general states $|\alpha\rangle$ and $|\beta\rangle$, we have the identity $\langle \beta | \mathcal{O} | \alpha \rangle = \langle \alpha | \mathcal{O}^\dagger | \beta \rangle^*$. On the Keldysh contour, $\langle \mathcal{O}^\dagger \rangle = \langle \mathcal{O} \rangle^*$, and (A.10) thus reduces to

$$\frac{\partial n_k}{\partial t} = 4 \text{Im} \int \prod_{i=2}^4 d^d k_i \lambda_{k234} \langle a_k^\dagger a_2^\dagger a_3 a_4 \rangle(t), \quad (\text{A.11})$$

which corresponds to (3.1) in the main text. The equal-time four-point function $\langle a_1^\dagger a_2^\dagger a_3 a_4 \rangle$ can be evaluated using either $a_k^+ = \frac{1}{\sqrt{2}}(A_k + \eta_k)$ or $a_k^- = \frac{1}{\sqrt{2}}(A_k - \eta_k)$; the result should be independent of the choice. Indeed, using four a^+ operators as an example,

$$\langle a_1^\dagger a_2^\dagger a_3 a_4 \rangle = \langle a_1^{+\dagger} a_2^{+\dagger} a_3^+ a_4^+ \rangle = \frac{1}{4} \langle A_1^\dagger A_2^\dagger A_3 A_4 \rangle. \quad (\text{A.12})$$

The last equality holds because equal-time correlators involving any number of η fields, such as e.g. $\langle A_1^\dagger \eta_2^\dagger A_3 A_4 \rangle$, vanish due to conflicting time orderings imposed by the retarded and advanced Green's functions, $G^A(t, t')G^R(t', t) = 0$. This demonstrates the last equality in (3.1).

B. Perturbative computation of equal-time correlation functions

In this appendix, we compute the equal-time four-point function entering the kinetic equation directly using perturbation theory, to second order. This is essentially the same derivation as in the main body of the text, but it doesn't make use of the path integral or the Keldysh contour. This provides a complementary perspective on the derivation and the result. Of course, beyond one loop the path integral approach in the main body is more efficient.⁴

We will work in the interaction picture: the operators evolve with the free Hamiltonian,

$$a_k(t) = e^{iH_0(t-t_0)} a_k e^{-iH_0(t-t_0)}, \quad (\text{B.1})$$

while the state evolves with the interaction Hamiltonian, and at time t is given by

$$|\Psi(t)\rangle = U(t, t_0)|\Psi(t_0)\rangle, \quad (\text{B.2})$$

where the initial state $|\Psi(t_0)\rangle$ is one in which mode k has occupation number n_k , i.e., it is a product of harmonic oscillator states $|n_k\rangle$ for each mode k . The evolution operator is given by,

$$U(t, t_0) = T \exp\left(-i \int_{t_0}^t dt' H_{int}(t')\right) = 1 - i \int_{t_0}^t dt_a H_{int}(t_a) - \int_{t_0}^t dt_a \int_{t_0}^{t_a} dt_b H_{int}(t_a) H_{int}(t_b) + \dots \quad (\text{B.3})$$

where T denotes time ordering, meaning that operators at later times appear further to the left.

We would like to compute the equal-time four-point function $\langle a_1^\dagger a_2^\dagger a_3 a_4 \rangle$, where the operator is at time t . Denoting

$$V_{1234}(t) \equiv a_1^\dagger(t) a_2^\dagger(t) a_3(t) a_4(t) \quad (\text{B.4})$$

so that $H_{int} = \sum_{1,2,3,4} \lambda_{1234} V_{1234}$ we need to compute,

$$\langle a_1^\dagger a_2^\dagger a_3 a_4 \rangle \equiv \langle \Psi(t) | V_{1234}(t) | \Psi(t) \rangle = \langle \Psi(t_0) | U(t, t_0)^\dagger V_{1234}(t) U(t, t_0) | \Psi(t_0) \rangle \quad (\text{B.5})$$

This is, of course, the Keldysh contour procedure used in the main text: the $U(t, t_0)$ is the portion of the contour running forwards in time, while $U(t, t_0)^\dagger$ runs backwards in time. Here, we will perform the computation explicitly to the first two orders, without using Feynman rules or propagators.

⁴A similar, but perhaps more involved, approach to the one in this appendix – perturbatively solving the Heisenberg equation for the density matrix – was discussed in [57]. For an equal-time approach, more similar to the one in this paper, see [58].

To order λ we get,

$$\begin{aligned} \langle a_1^\dagger a_2^\dagger a_3 a_4 \rangle &= -i \int_{t_0}^t dt' (\langle \Psi(t_0) | V_{1234}(t) H_{int}(t') | \Psi(t_0) \rangle - \langle \Psi(t_0) | H_{int}(t') V_{1234}(t) | \Psi(t_0) \rangle) + \dots \\ &= -4i \lambda_{3412} \int_{t_0}^t dt' (\langle \Psi(t_0) | V_{1234}(t) V_{3412}(t') | \Psi(t_0) \rangle - \langle \Psi(t_0) | V_{3412}(t') V_{1234}(t) | \Psi(t_0) \rangle) + \dots \end{aligned} \quad (\text{B.6})$$

We note that the action of an annihilation operator for a single mode (B.1) on the initial state is

$$a_k(t) |n_k\rangle = e^{i\omega_k(n_k-1)(t-t_0)} \sqrt{n_k} e^{-i\omega_k n_k(t-t_0)} |n_k-1\rangle = e^{-i\omega_k(t-t_0)} \sqrt{n_k} |n_k-1\rangle \quad (\text{B.7})$$

since the energy of the free system before a_k acts is $\omega_k n_k$, whereas after a_k acts, it is $\omega_k(n_k-1)$. Thus, we obtain,

$$\begin{aligned} \int_{t_0}^t dt' \langle \Psi(t_0) | V_{1234}(t) V_{3412}(t') | \Psi(t_0) \rangle &= n_1 n_2 (n_3+1) (n_4+1) e^{i\omega_{12;34}(t-t_0)} \int_{t_0}^t dt' e^{i\omega_{34;12}(t'-t_0)} \\ &= -i \frac{n_1 n_2 (n_3+1) (n_4+1)}{\omega_{34;12} - i\epsilon} \end{aligned} \quad (\text{B.8})$$

Therefore, (B.6) reproduces the tree-level answer (3.4).

At second order, there are three terms:

1.
$$- \int_{t_0}^t dt_a \int_{t_0}^{t_a} dt_b \langle \Psi(t_0) | V_{1234}(t) H_{int}(t_a) H_{int}(t_b) | \Psi(t_0) \rangle \quad (\text{B.9})$$

2.
$$- \int_{t_0}^t dt_a \int_{t_0}^{t_a} dt_b \langle \Psi(t_0) | H_{int}(t_b) H_{int}(t_a) V_{1234}(t) | \Psi(t_0) \rangle \quad (\text{B.10})$$

3.
$$\int_{t_0}^t dt_a \int_{t_0}^t dt_b \langle \Psi(t_0) | H_{int}(t_a) V_{1234}(t) H_{int}(t_b) | \Psi(t_0) \rangle \quad (\text{B.11})$$

We will first focus on obtaining the s -channel four-point function. Starting with the first term, we see that the two H_{int} must be V_{5612} and V_{3456} , with the only choice being which one is at time t_a and which is at t_b . So (B.9) becomes,

$$\begin{aligned} -16 \lambda_{3456} \lambda_{5612} \int_{t_0}^t dt_a \int_{t_0}^{t_a} dt_b (\langle \Psi(t_0) | V_{1234}(t) V_{5612}(t_a) V_{3456}(t_b) | \Psi(t_0) \rangle + \langle \Psi(t_0) | V_{1234}(t) V_{3456}(t_a) V_{5612}(t_b) | \Psi(t_0) \rangle) \\ = 16 \lambda_{3456} \lambda_{5612} \frac{n_1 n_2 (n_3+1) (n_4+1)}{\omega_{34;12} - i\epsilon} \left(\frac{n_5 n_6}{\omega_{34;56} - i\epsilon} + \frac{(n_5+1)(n_6+1)}{\omega_{56;12} - i\epsilon} \right) \end{aligned} \quad (\text{B.12})$$

Likewise, (B.10) becomes

$$\begin{aligned}
& -16\lambda_{3456}\lambda_{5612} \int_{t_0}^t dt_a \int_{t_0}^{t_a} dt_b \left(\langle \Psi(t_0) | V_{5612}(t_b) V_{3456}(t_a) V_{1234}(t) | \Psi(t_0) \rangle + \langle \Psi(t_0) | V_{3456}(t_b) V_{5612}(t_a) V_{1234}(t) | \Psi(t_0) \rangle \right) \\
& = 16\lambda_{3456}\lambda_{5612} \frac{(n_1+1)(n_2+1)n_3n_4}{\omega_{34;12}-i\epsilon} \left(\frac{n_5n_6}{\omega_{56;12}-i\epsilon} + \frac{(n_5+1)(n_6+1)}{\omega_{34;56}-i\epsilon} \right) \quad (\text{B.13})
\end{aligned}$$

Finally, for (B.11), there is no time ordering and we get,

$$\begin{aligned}
& 16\lambda_{3456}\lambda_{5612} \int_{t_0}^t dt_a \int_{t_0}^t dt_b \left(\langle \Psi(t_0) | V_{5612}(t_a) V_{1234}(t) V_{3456}(t_b) | \Psi(t_0) \rangle + \langle \Psi(t_0) | V_{3456}(t_a) V_{1234}(t) V_{5612}(t_b) | \Psi(t_0) \rangle \right) \\
& = -16\lambda_{3456}\lambda_{5612} \frac{(n_1+1)(n_2+1)(n_3+1)(n_4+1)n_5n_6 + n_1n_2n_3n_4(n_5+1)(n_6+1)}{(\omega_{34;56}-i\epsilon)(\omega_{56;12}-i\epsilon)} \quad (\text{B.14}) \\
& = -16\lambda_{3456}\lambda_{5612} \frac{(n_1+1)(n_2+1)(n_3+1)(n_4+1)n_5n_6 + n_1n_2n_3n_4(n_5+1)(n_6+1)}{\omega_{34;12}-i\epsilon} \left(\frac{1}{\omega_{34;56}-i\epsilon} + \frac{1}{\omega_{56;12}-i\epsilon} \right)
\end{aligned}$$

where in the last equality we rewrote the ω denominators in a way that will be convenient in what we do next.

Let us combine the terms from (B.12), (B.13), (B.14) that have $\omega_{34;56}$ in the denominator. This gives,

$$\begin{aligned}
& \frac{16\lambda_{3456}\lambda_{5612}}{(\omega_{34;12}-i\epsilon)(\omega_{34;56}-i\epsilon)} \left(n_1n_2(n_3+1)(n_4+1)n_5n_6 + (n_1+1)(n_2+1)n_3n_4(n_5+1)(n_6+1) \right. \\
& \quad \left. - (n_1+1)(n_2+1)(n_3+1)(n_4+1)n_5n_6 - n_1n_2n_3n_4(n_5+1)(n_6+1) \right) \quad (\text{B.15})
\end{aligned}$$

Combining the numerators factors precisely reproduces what we had in (3.14). The same applies to the terms with $\omega_{56;12}$ in the denominator. We thus recover the s -channel contribution to the four-point function at one loop, given in (3.14). The t -channel contribution is obtained from (B.9–B.11) by letting one of the H_{int} have a V_{3516} and the other a V_{4625} .

C. Particle number non-conserving interactions

While the main body of the text dealt with quartic interactions involving two creation and two annihilation operators (2.4), this can be easily generalized to cubic or higher-order interactions, as well as interactions with an unequal number of creation and annihilation operators.

Cubic Interaction

For instance, consider a cubic interaction,

$$H_{int} = \frac{1}{2} \int \prod_{i=1}^3 d^d k_i \lambda_{123} a_{k_1}^\dagger a_{k_2} a_{k_3} \delta(\vec{k}_{1;23}) + \text{h.c.} \quad (\text{C.1})$$

From (2.13), we have that on the Keldysh contour, $L_{int} = -H_{int}(a^+) + H_{int}(a^-)$. Rotating to the A and η fields (2.14) gives,

$$L_{int} = -\frac{1}{2\sqrt{2}} \int \prod_{i=1}^3 d^d k_i \lambda_{123} \left(\eta_1^\dagger \eta_2 \eta_3 + \eta_1^\dagger A_2 A_3 + 2A_1^\dagger A_2 \eta_3 \right) + \text{h.c.} . \quad (\text{C.2})$$

Computing the tree-level, equal-time three-point function,

$$\begin{aligned} \langle A_1^\dagger A_2 A_3 \rangle_{\text{tree}} &= \frac{1}{\sqrt{2}} \lambda_{123}^* \left(1 + (2n_2+1)(2n_3+1) - (2n_1+1)(2n_2+1) + (2n_1+1)(2n_3+1) \right) \frac{1}{\omega_{23;1} - i\epsilon} \\ &= 2\sqrt{2} \lambda_{123}^* \left(n_2 n_3 (1+n_1) - n_1 (1+n_2)(1+n_3) \right) \frac{1}{\omega_{23;1} - i\epsilon} , \end{aligned} \quad (\text{C.3})$$

where in the first equality, the first term in parentheses (the 1) originates from the Hermitian conjugate of the first term (η^3) in (C.2), while the second and third terms arise from the Hermitian conjugate of the second and third terms in (C.2), respectively. The kinetic equation is expressed in terms of the correlator as,

$$\frac{\partial n_k}{\partial t} = \text{Im} \int \prod_{i=1}^3 d^d k_i (\delta_{kk_1} - \delta_{kk_2} - \delta_{kk_3}) \lambda_{123} \langle a_{k_1}^\dagger a_{k_2} a_{k_3} \rangle \delta(\vec{k}_{1;23}) , \quad (\text{C.4})$$

where $\delta_{kk_i} \equiv \delta(\vec{k} - \vec{k}_i)$. Using the three-point function (C.3), this gives

$$\frac{\partial n_k}{\partial t} = \pi \int \prod_{i=1}^3 d^d k_i |\lambda_{123}|^2 (\delta_{kk_1} - \delta_{kk_2} - \delta_{kk_3}) \delta(\omega_{1;23}) \delta(\vec{k}_{1;23}) \left((1+n_1)n_2n_3 - n_1(1+n_2)(1+n_3) \right) \quad (\text{C.5})$$

Quartic interaction

Now consider a quartic interaction, but one that has three creation operators and one annihilation operator,

$$H_{int} = \frac{1}{2} \int \prod_{i=1}^4 d^d k_i \lambda_{1;234} a_{k_1}^\dagger a_{k_2} a_{k_3} a_{k_4} \delta(\vec{k}_{1;234}) + \text{h.c.} . \quad (\text{C.6})$$

From (2.13), we have that on the Keldysh contour, $L_{int} = -H(a^+) + H(a^-)$. Rotating to the A and η fields (2.14) gives

$$L_{int} = -\frac{1}{4} \int \prod_{i=1}^4 d^d k_i \lambda_{1;234} \left(\eta_1^\dagger A_2 A_3 A_4 + 3A_1^\dagger A_2 \eta_3 A_4 + A_1^\dagger \eta_2 \eta_3 \eta_4 + 3\eta_1^\dagger \eta_2 A_3 \eta_4 \right) + \text{h.c.} . \quad (\text{C.7})$$

The correlator is then,

$$\langle A_1^\dagger A_2 A_3 A_4 \rangle_{\text{tree}} = 12 \lambda_{1;234}^* \left((1+n_1)n_2n_3n_4 - n_1(1+n_2)(1+n_3)(1+n_4) \right) \frac{1}{\omega_{234;1} - i\epsilon} , \quad (\text{C.8})$$

which, upon inserting into,

$$\frac{\partial n_k}{\partial t} = \text{Im} \int \prod_{i=1}^4 d^d k_i (\delta_{kk_1} - 3\delta_{kk_2}) \lambda_{1;234} \langle a_{k_1}^\dagger a_{k_2} a_{k_3} a_{k_4} \rangle \quad (\text{C.9})$$

gives the tree-level kinetic equation,

$$\frac{\partial n_k}{\partial t} = 3\pi \int \prod_{i=1}^4 d^d k_i |\lambda_{1;234}|^2 (\delta_{kk_1} - 3\delta_{kk_2}) \delta(\omega_{1;234}) \delta(\vec{k}_{1;234}) \left((1+n_1)n_2n_3n_4 - n_1(1+n_2)(1+n_3)(1+n_4) \right) \quad (\text{C.10})$$

In fact, we could have obtained this more simply from the kinetic equation with the particle number conserving quartic interaction (3.6),

$$\frac{\partial n_k}{\partial t} = 4\pi \int \prod_{i=1}^4 d^d k_i |\lambda_{1234}|^2 (\delta_{kk_1} + \delta_{kk_2} - \delta_{kk_3} - \delta_{kk_4}) \left((1+n_1)(1+n_2)n_3n_4 - n_1n_2(1+n_3)(1+n_4) \right) \delta(\omega_{12;34}) \delta(\vec{k}_{12;34}) \quad (\text{C.11})$$

by sending $2 \rightarrow -2$, which corresponds to $n_2 \rightarrow -1-n_2$ (and accounting for an overall minus sign, and the change in the prefactor).

C.1. Next-to-leading order kinetic equation for $\lambda\phi^4$ theory

The bulk of the paper focused on interactions of the form (2.4), which have a definite number of creation and annihilation operators. We may easily extend this to interactions that are sums of such terms. Here we consider the case of relativistic $\lambda\phi^4$ field theory, having the interaction (2.3). This interaction contains, in addition to 2 to 2 scattering, scattering that is 3 to 1 or 4 to 0. At tree level these other terms are irrelevant, since 3 to 1 scattering is not possible for a relativistic scalar with the dispersion relation $\omega_k = \sqrt{\vec{k}^2 + m^2}$. The only diagram is the one shown in Fig. 6(a). At one-loop level, on the other hand, these other interactions can appear and are shown in Fig. 6.

As one sees from (2.1) and (2.3), the interaction λ_{1234} for $\lambda\phi^4$ theory is,

$$\lambda_{1234} = \frac{\lambda}{16\sqrt{\omega_{k_1}\omega_{k_2}\omega_{k_3}\omega_{k_4}}} \quad (\text{C.12})$$

We find that the next-to-leading-order kinetic equation is,

$$\omega_1 \frac{\partial n_1}{\partial t} = \frac{\pi\lambda^2}{16} \int \frac{d^d k_2}{\omega_2} \frac{d^d k_3}{\omega_3} \frac{d^d k_4}{\omega_4} \left((n_1+1)(n_2+1)n_3n_4 - n_1n_2(n_3+1)(n_4+1) \right) \left(1 + 2(\mathcal{L}_+ + 2\bar{\mathcal{L}}_+ + \tilde{\mathcal{L}}_+) + 4(2\mathcal{L}_- + \bar{\mathcal{L}}_- + \tilde{\mathcal{L}}_-) \right) \delta(\omega_{12;34}) \delta(\vec{k}_{12;34}) \quad (\text{C.13})$$

Here, the additional loop integrals account for some of the interactions being 3 to 1 or 4 to 0.

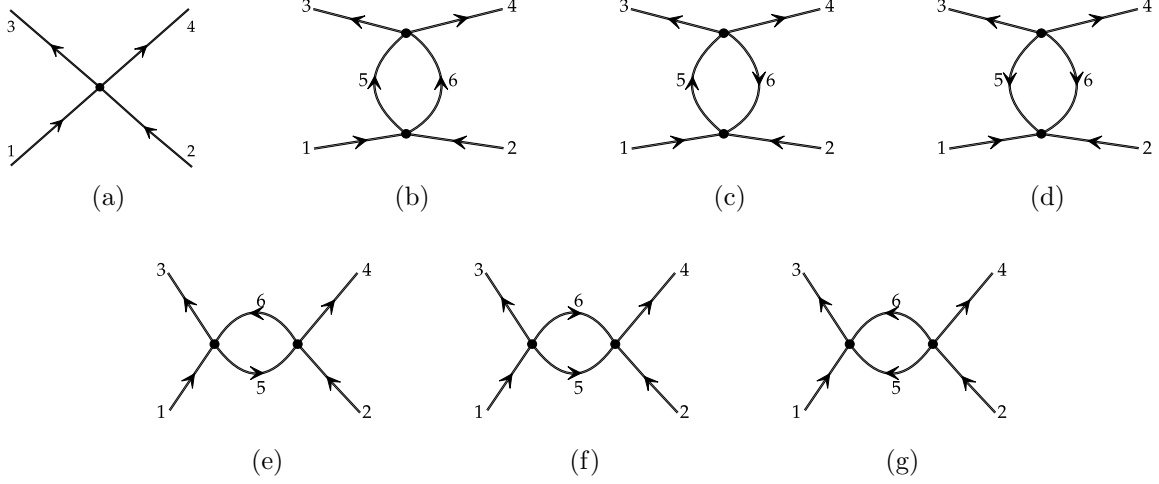


Figure 6: Diagrams for the $\langle a_1^\dagger a_2^\dagger a_3 a_4 \rangle$ four-point function in $\lambda\phi^4$ theory. (a) tree-level. One-loop: (b) \mathcal{L}_+ , (c) $\bar{\mathcal{L}}_+$, (d) $\tilde{\mathcal{L}}_+$, (e) \mathcal{L}_- , (f) $\bar{\mathcal{L}}_-$, (g) $\tilde{\mathcal{L}}_-$.

Namely, the loop integrals \mathcal{L}_\pm which we had before (and correspond to 2 to 2 scattering), see (3.18) are,

$$\mathcal{L}_+ = 2\lambda \int \frac{d^d k_5}{2\omega_5} \frac{d^d k_6}{2\omega_6} \frac{n_5+n_6+1}{\omega_{12;56}} \delta(\vec{k}_{12;56}), \quad \mathcal{L}_- = 2\lambda \int \frac{d^d k_5}{2\omega_5} \frac{d^d k_6}{2\omega_6} \frac{n_6-n_5}{\omega_{16;35}} \delta(\vec{k}_{16;35}). \quad (\text{C.14})$$

The diagram \mathcal{L}_+^1 corresponds to replacing the 2 to 2 interaction in \mathcal{L}_+ with a 3 to 1 interaction, which we achieve by flipping the arrows on 6, while \mathcal{L}_+^0 corresponds to having a 4 to 0 interaction, which we achieve by flipping both the 5 and 6 arrows on \mathcal{L}_+^2 ,

$$\bar{\mathcal{L}}_+ = 2\lambda \int \frac{d^d k_5}{2\omega_5} \frac{d^d k_6}{2\omega_6} \frac{n_6-n_5}{\omega_{126;5}} \delta(\vec{k}_{126;5}), \quad \tilde{\mathcal{L}}_+ = -2\lambda \int \frac{d^d k_5}{2\omega_5} \frac{d^d k_6}{2\omega_6} \frac{n_5+n_6+1}{\omega_{1256}} \delta(\vec{k}_{1256}), \quad (\text{C.15})$$

where $\omega_{126;5} \equiv \omega_1+\omega_2+\omega_6-\omega_5$ and $\omega_{1256} \equiv \omega_1+\omega_2+\omega_5+\omega_6$. We may similarly take \mathcal{L}_- and flip the arrows on 6, giving $\bar{\mathcal{L}}_-$, or instead on 5, giving $\tilde{\mathcal{L}}_-$. Both of these have 3 to 1 interactions,

$$\bar{\mathcal{L}}_- = 2\lambda \int \frac{d^d k_5}{2\omega_5} \frac{d^d k_6}{2\omega_6} \frac{1+n_5+n_6}{\omega_{1;356}} \delta(\vec{k}_{1;356}), \quad \tilde{\mathcal{L}}_- = -2\lambda \int \frac{d^d k_5}{2\omega_5} \frac{d^d k_6}{2\omega_6} \frac{1+n_5+n_6}{\omega_{156;3}} \delta(\vec{k}_{156;3}). \quad (\text{C.16})$$

Manifest Lorentz invariance

Let us rewrite (C.13) in a way that makes the underlying Lorentz invariance of the theory manifest. We perform variable changes to rewrite the loop integrals as,

$$\mathcal{L}_+ = \lambda \int \frac{d^d k_5}{\omega_5 \omega_6} \frac{n_5+\frac{1}{2}}{\omega_{12;56}}, \quad \bar{\mathcal{L}}_+ = \frac{\lambda}{2} \int \frac{d^d k_5 (n_5+\frac{1}{2})}{\omega_5 \omega_6} \left(\frac{1}{\omega_{125;6}} - \frac{1}{\omega_{126;5}} \right), \quad \tilde{\mathcal{L}}_+ = -\lambda \int \frac{d^d k_5}{\omega_5 \omega_6} \frac{n_5+\frac{1}{2}}{\omega_{1256}},$$

where $\vec{k}_6 = \vec{k}_1 + \vec{k}_2 - \vec{k}_5$ for all the terms. As a result,

$$\mathcal{L}_+ + 2\bar{\mathcal{L}}_+ + \tilde{\mathcal{L}}_+ = 2\lambda \int \frac{d^d k_5 (n_5 + \frac{1}{2})}{\omega_5} \left(\frac{1}{\omega_{12;5}^2 - \omega_6^2} + \frac{1}{\omega_{125}^2 - \omega_6^2} \right). \quad (\text{C.17})$$

Likewise,

$$\mathcal{L}_- = \frac{\lambda}{2} \int \frac{d^d k_5 (n_5 + \frac{1}{2})}{\omega_5 \omega_6} \left(\frac{1}{\omega_{15;36}} - \frac{1}{\omega_{16;35}} \right), \quad \bar{\mathcal{L}}_- = \lambda \int \frac{d^d k_5 n_5 + \frac{1}{2}}{\omega_5 \omega_6 \omega_{1;356}}, \quad \tilde{\mathcal{L}}_- = -\lambda \int \frac{d^d k_5 n_5 + \frac{1}{2}}{\omega_5 \omega_6 \omega_{156;3}},$$

where $\vec{k}_6 = \vec{k}_1 - \vec{k}_3 - \vec{k}_5$ for all the terms. As a result,

$$2\mathcal{L}_- + \bar{\mathcal{L}}_- + \tilde{\mathcal{L}}_- = 2\lambda \int \frac{d^d k_5 (n_5 + \frac{1}{2})}{\omega_5} \left(\frac{1}{\omega_{1;35}^2 - \omega_6^2} + \frac{1}{\omega_{15;3}^2 - \omega_6^2} \right). \quad (\text{C.18})$$

Therefore, we can rewrite (C.13) as [54]

$$\omega_{|\mathbf{k}_1|} \frac{\partial n_1}{dt} = \frac{\pi \lambda^2}{16} \int \frac{d\mathbf{k}_2}{\omega_{|\mathbf{k}_2|}} \frac{d\mathbf{k}_3}{\omega_{|\mathbf{k}_3|}} \frac{d\mathbf{k}_4}{\omega_{|\mathbf{k}_4|}} \left[(n_1 + 1)(n_2 + 1)n_3 n_4 - n_1 n_2 (n_3 + 1)(n_4 + 1) \right. \\ \left. \left(1 + 2\mathcal{L}(k_1 + k_2) + 4\mathcal{L}(k_1 - k_3) \right) \delta(\omega_{|\mathbf{k}_1|} + \omega_{|\mathbf{k}_2|} - \omega_{|\mathbf{k}_3|} - \omega_{|\mathbf{k}_4|}) \delta(\mathbf{k}_1 + \mathbf{k}_2 - \mathbf{k}_3 - \mathbf{k}_4) \right], \quad (\text{C.19})$$

where k is a four-vector, with time component k^0 and spatial component \mathbf{k} , and

$$\mathcal{L}(k) = \lambda \int d^d q \frac{(n_{\mathbf{q}} + \frac{1}{2})}{2\omega_{|\mathbf{q}|}} \left[\frac{1}{(k^0 - \omega_{|\mathbf{q}|})^2 - (\mathbf{k} - \mathbf{q})^2} + \frac{1}{(k^0 + \omega_{|\mathbf{q}|})^2 - (\mathbf{k} - \mathbf{q})^2} \right], \quad (\text{C.20})$$

which we may rewrite in terms of a $d+1$ spacetime dimension integral,

$$\mathcal{L}(k) = 2\lambda \int d^{d+1} q \frac{(n_{\mathbf{q}} + \frac{1}{2}) \delta(q^2 - m^2)}{(k - q)^2}, \quad (\text{C.21})$$

where we are using relativistic notation, $k^2 = k_0^2 - \mathbf{k}^2$.

The expression (C.19) naturally emerges from working with ϕ fields rather than with a fields. Namely, upon doing a field rotation, see e.g. [36, 37],

$$\phi = \frac{1}{2}(\phi^+ + \phi^-), \quad \eta = \phi^+ - \phi^-, \quad (\text{C.22})$$

the $\lambda\phi^4$ Lagrangian on the Keldysh contour takes the form,

$$\mathcal{L} = \partial\eta\partial\phi - \frac{\lambda}{3!}(\eta\phi^3 + \frac{1}{4}\eta^3\phi), \quad (\text{C.23})$$

and the Keldysh and retarded Green's functions take the form, respectively,

$$G_k^K = \langle \phi_k^* \phi_k \rangle = \delta(k^2 - m^2) \left(n_{\mathbf{k}} + \frac{1}{2} \right), \quad G_k^R = \langle \phi_k^* \eta_k \rangle = \frac{i}{k^2 - m^2 + i\epsilon k_0}. \quad (\text{C.24})$$

The Feynman diagrams now no longer have arrows and the one-loop contribution to the $\eta\phi^3$ vertex is given by

$$\lambda\mathcal{L}(k_1+k_2) + \lambda\mathcal{L}(k_1-k_3) + \lambda\mathcal{L}(k_1-k_4) \quad (\text{C.25})$$

where \mathcal{L} is given by (C.21) and contains a Keldysh propagator for one of the internal lines and a retarded propagator for the other (C.24). The u channel contribution is equivalent to the t channel contribution after a $3 \leftrightarrow 4$ variable change. Thus we get the one-loop kinetic equation (C.19).

References

- [1] R. L. Liboff, *Kinetic Theory: Classical, Quantum, and Relativistic Descriptions*. 2003. Springer.
- [2] E. W. Kolb and M. Turner, *The Early Universe*. Taylor and Francis, 1994.
- [3] K. Kawasaki and I. Oppenheim, “Logarithmic term in the density expansion of transport coefficients,” *Phys. Rev.* **139** (Sep, 1965) A1763–A1768.
- [4] J. R. Dorfman and E. G. D. Cohen, “Velocity correlation functions in two and three dimensions,” *Phys. Rev. Lett.* **25** (Nov, 1970) 1257–1260.
- [5] J. R. Dorfman, T. R. Kirkpatrick, and J. V. Sengers, “Why Non-equilibrium is Different,” [arXiv:1512.02679](https://arxiv.org/abs/1512.02679) [cond-mat.stat-mech].
- [6] J. R. Dorfman, H. van Beijeren, and T. R. Kirkpatrick, *Contemporary Kinetic Theory of Matter*. Cambridge University Press, 2021.
- [7] A. Shytov, J. F. Kong, G. Falkovich, and L. Levitov, “Particle collisions and negative nonlocal response of ballistic electrons,” *Phys. Rev. Lett.* **121** (Oct, 2018) 176805.
- [8] M. S. Green, “Boltzmann equation from the statistical mechanical point of view,” *The Journal of Chemical Physics* **25** (1956) no. 5, 836–855.
- [9] E. Cohen, “On the generalization of the boltzmann equation to general order in the density,” *Physica* **28** (1962) no. 10, 1025–1044.
- [10] R. Zwanzig, “Method for finding the density expansion of transport coefficients of gases,” *Physical Review* **129** (1963) no. 1, 486.

- [11] N. Bogoliubov, *Problems of Dynamic Theory in Statistical Physics*. Technical Information Service, United States Atomic Energy Commission, 1960.
- [12] J. Brocas, “On the comparison between two generalized boltzmann equations,” *Advances in Chemical Physics* (1967) 317–381.
- [13] R. Balescu, “Irreversible processes in ionized gases,” *The Physics of Fluids* **3** (1960) no. 1, 52–63.
- [14] I. Prigogine, *Non-equilibrium Statistical Mechanics*. Interscience Publishers, 1962. Reprint: Dover Publications, 2017.
- [15] V. Rosenhaus and M. Smolkin, “Feynman rules for forced wave turbulence,” *JHEP* **01** (2023) 142, [arXiv:2203.08168](https://arxiv.org/abs/2203.08168) [`cond-mat.stat-mech`].
- [16] V. Rosenhaus and M. Smolkin, “Wave turbulence and the kinetic equation beyond leading order,” *Phys. Rev. E* **109** (2024) no. 6, 064127, [arXiv:2212.02555](https://arxiv.org/abs/2212.02555) [`cond-mat.stat-mech`].
- [17] V. Rosenhaus, D. Schubring, M. S. J. Shuvo, and M. Smolkin, “Loop diagrams in the kinetic theory of waves,” *JHEP* **06** (2024) 025, [arXiv:2308.00740](https://arxiv.org/abs/2308.00740) [`hep-th`].
- [18] V. E. Zakharov, V. S. L’vov, and G. Falkovich, *Kolmogorov Spectra of Turbulence I: Wave Turbulence*. Springer-Verlag, 1992.
- [19] M. Onorato and G. Dematteis, “A straightforward derivation of the four-wave kinetic equation in action-angle variables,” *Journal of Physics Communications* **4** (2020) no. 9, 095016, [arXiv:1911.13057](https://arxiv.org/abs/1911.13057) [`nlin.CD`].
- [20] V. E. Zakharov and V. S. Lvov, “The statistical description of nonlinear wave fields,” *Radiophysics and Quantum Electronics* **18** (1975) no. 10, 1470–1487. <https://link.springer.com/content/pdf/10.1007/BF01040337.pdf>.
- [21] Y. Deng and Z. Hani, “Long time justification of wave turbulence theory,” [arXiv:2311.10082](https://arxiv.org/abs/2311.10082) [`math.AP`].
- [22] Y. Deng, Z. Hani, and X. Ma, “Hilbert’s sixth problem: derivation of fluid equations via Boltzmann’s kinetic theory,” [arXiv:2503.01800](https://arxiv.org/abs/2503.01800) [`math.AP`].
- [23] S. Mrowczynski and P. Danielewicz, “Green Function Approach to Transport Theory of Scalar Fields,” *Nucl. Phys. B* **342**, 345-380 (1990).
- [24] M. E. Carrington and S. Mrowczynski, “Transport theory beyond binary collisions,” *Phys. Rev. D* **71**, 065007 (2005).

- [25] F. Fillion-Gourdeau, J. S. Gagnon and S. Jeon, “All orders Boltzmann collision term from the multiple scattering expansion of the self-energy,” *Phys. Rev. D* **74**, 025010 (2006), [arXiv:hep-ph/0603212](#).
- [26] S. Weinstock, “Boltzmann collision term,” *Phys. Rev. D* **73**, 025005 (2006), [arXiv:hep-ph/0510417](#).
- [27] A. Kamenev, *Field Theory of Non-Equilibrium Systems*. Cambridge University Press, 2011.
- [28] E. A. Calzetta and B. L. Hu, *Nonequilibrium Quantum Field Theory*. Cambridge University Press, 2009.
- [29] P. B. Arnold, D. T. Son, and L. G. Yaffe, “Effective dynamics of hot, soft nonAbelian gauge fields. Color conductivity and $\log(1/\alpha)$ effects,” *Phys. Rev. D* **59** (1999) 105020, [arXiv:hep-ph/9810216](#).
- [30] C. R. Galley, “Classical Mechanics of Nonconservative Systems,” *Phys. Rev. Lett.* **110** (2013) no. 17, 174301, [arXiv:1210.2745 \[gr-qc\]](#).
- [31] C. R. Galley, D. Tsang, and L. C. Stein, “The principle of stationary nonconservative action for classical mechanics and field theories,” [arXiv:1412.3082 \[math-ph\]](#).
- [32] P. C. Martin, E. Siggia, and H. A. Rose, “Statistical Dynamics of Classical Systems,” *Phys. Rev. A* **8** (1973) no. 1, 423–437.
- [33] C. de Dominicis, “Techniques of field renormalization and dynamics of critical phenomena,” *J. Phys. (Paris)* **37** (1976) C1.
- [34] H. Janssen, “On a lagrangean for classical field dynamics and renormalization group calculations of dynamical critical properties,” *Z. Physik* **23** (1976) 377.
- [35] F. M. Haehl, R. Loganayagam and M. Rangamani, “Schwinger-Keldysh formalism. Part I: BRST symmetries and superspace,” *JHEP* **06**, 069 (2017) .
- [36] A. H. Mueller and D. T. Son, “On the Equivalence between the Boltzmann equation and classical field theory at large occupation numbers,” *Phys. Lett. B* **582** (2004) 279–287, [arXiv:hep-ph/0212198](#).
- [37] S. Jeon, “The Boltzmann equation in classical and quantum field theory,” *Phys. Rev. C* **72** (2005) 014907, [arXiv:hep-ph/0412121](#).
- [38] X.-Y. Hu and V. Rosenhaus, “Random coupling model of turbulence as a classical Sachdev-Ye-Kitaev model,” *Phys. Rev. E* **108** (2023) no. 5, 054132, [arXiv:2303.03421 \[hep-th\]](#).

- [39] A. Newell and V. Zakharov, “The role of the generalized Phillips’ spectrum in wave turbulence,” *Physics Letters A* **372** (2008) no. 23, 4230–4233.
- [40] M. Shavit, O. Bühler, and J. Shatah, “Turbulent spectrum of 2d internal gravity waves,” *Phys. Rev. Lett.* **134** (Feb, 2025) 054101.
- [41] E. Falcon and N. Mordant, “Experiments in Surface Gravity – Capillary Wave Turbulence,” *Annual Review of Fluid Mechanics* **54** (Jan, 2022) 1–25, [arXiv:2107.04015](https://arxiv.org/abs/2107.04015) [[physics.flu-dyn](https://arxiv.org/archive/physics)].
- [42] E. A. Kochurin and P. A. Russkikh, “Plane-Symmetric Capillary Turbulence: Five-Wave Interactions,” [arXiv:2501.18970](https://arxiv.org/abs/2501.18970) [[physics.flu-dyn](https://arxiv.org/archive/physics)].
- [43] N. Navon, C. Eigen, J. Zhang, R. Lopes, A. L. Gaunt, K. Fujimoto, M. Tsubota, R. P. Smith, and Z. Hadzibabic, “Synthetic dissipation and cascade fluxes in a turbulent quantum gas,” *Science* **366** (Oct., 2019) .
- [44] L. H. Dogra, G. Martirosyan, T. A. Hilker, J. A. P. Glidden, J. Etrych, A. Cao, C. Eigen, R. P. Smith, and Z. Hadzibabic, “Universal equation of state for wave turbulence in a quantum gas,” *Nature* **620** (July, 2023) .
- [45] B. Nowak, J. Schole, D. Sexty, and T. Gasenzer, “Nonthermal fixed points, vortex statistics, and superfluid turbulence in an ultracold Bose gas,” *Phys. Rev. A* **85** (2012) 043627, [arXiv:1111.6127](https://arxiv.org/abs/1111.6127) [[cond-mat.quant-gas](https://arxiv.org/archive/cond-mat)].
- [46] Y. Zhu, B. Semisalov, G. Krstulovic, and S. Nazarenko, “Self-similar evolution of wave turbulence in gross-pitaevskii system,” *Phys. Rev. E* **108** (Dec., 2023) .
- [47] Y. Zhu, G. Krstulovic, and S. Nazarenko, “Transition to strong wave turbulence in Bose-Einstein condensates,” [arXiv:2411.19812](https://arxiv.org/abs/2411.19812) [[cond-mat.quant-gas](https://arxiv.org/archive/cond-mat)].
- [48] V. Rosenhaus and G. Falkovich, “Weak and strong turbulence in self-focusing and defocusing media,” [arXiv:2501.12451](https://arxiv.org/abs/2501.12451) [[physics.flu-dyn](https://arxiv.org/archive/physics)].
- [49] V. Noel, T. Gasenzer, and K. Boguslavski, “Kelvin waves in nonequilibrium universal dynamics of relativistic scalar field theories,” [arXiv:2503.01771](https://arxiv.org/abs/2503.01771) [[cond-mat.quant-gas](https://arxiv.org/archive/cond-mat)].
- [50] R. Micha and I. I. Tkachev, “Turbulent thermalization,” *Phys. Rev. D* **70** (2004) 043538, [arXiv:hep-ph/0403101](https://arxiv.org/abs/hep-ph/0403101).
- [51] S. M. D. Gregory, S. Schiattarella, V. S. Barroso, D. I. Kaiser, A. Avgoustidis, and S. Weinfurtner, “Tracing the nonlinear formation of an interfacial wave spectral cascade from one to few to many,” [arXiv:2410.08842](https://arxiv.org/abs/2410.08842) [[gr-qc](https://arxiv.org/archive/gr)].

- [52] J. Berges, M. P. Heller, A. Mazeliauskas, and R. Venugopalan, “QCD thermalization: Ab initio approaches and interdisciplinary connections,” *Rev. Mod. Phys.* **93** (2021) no. 3, 035003, [arXiv:2005.12299 \[hep-th\]](#).
- [53] A. Piñeiro Orioli, K. Boguslavski, and J. Berges, “Universal self-similar dynamics of relativistic and nonrelativistic field theories near nonthermal fixed points,” *Phys. Rev. D* **92** (2015) no. 2, 025041, [arXiv:1503.02498 \[hep-ph\]](#).
- [54] R. Walz, K. Boguslavski, and J. Berges, “Large- N kinetic theory for highly occupied systems,” *Phys. Rev. D* **97** (2018) no. 11, 116011, [arXiv:1710.11146 \[hep-ph\]](#).
- [55] I. Chantesana, A. Piñeiro Orioli, and T. Gasenzer, “Kinetic theory of nonthermal fixed points in a Bose gas,” *Phys. Rev. A* **99** (2019) no. 4, 043620, [arXiv:1801.09490 \[cond-mat.quant-gas\]](#).
- [56] V. Rosenhaus and D. Schubring, “Strong wave turbulence in strongly local large N theories,” [arXiv:2406.18475 \[hep-th\]](#).
- [57] D. W. Snoke, G.-Q. Liu, and S. M. Girvin, “The basis of the Second Law of thermodynamics in quantum field theory,” *Annals Phys.* **327** (2012) 1825–1851, [arXiv:1112.3009 \[cond-mat.stat-mech\]](#).
- [58] R. Ott, T. V. Zache, and J. Berges, “Equal-time approach to real-time dynamics of quantum fields,” *SciPost Phys.* **14** (2023) no. 2, 011, [arXiv:2204.06463 \[cond-mat.quant-gas\]](#).